Contribution from the Department of Medicinal Chemistry, Hiroshima University School of Medicine, Kasumi, Hiroshima 734, Japan, and the Departments of Chemistry, College of General Education, Hirosaki University, Bunkyo, Hirosaki 036, Japan, and Ehime University, Bunkyo, Matsuyama 790, Japan

A New Pyridyl-Containing Pentaaza Macrocyclic Ligand. Stabilization in Aqueous Solutions of the Iron(II) Complex and Its Dioxygen Adduct

EIICHI KIMURA,*[1a] MUTSUO KODAMA,[1b] RYOSUKE MACHIDA,[1a] and KAZUHIKO ISHIZU[1c]

Received May 29, 1981

A new macrocyclic pentadentate ligand, pyridyl-containing 16-membered pentaamine (L^1), greatly stabilizes a violet-pink-colored oxygenated species of iron(II) in aqueous solutions at room temperature; this ligand could be formulated as a 2:1 $(FeL^{2+})_2$–O_2 adduct by O_2 uptake measurements and pH metric titrations. The O_2 uptake stoichiometry and the violet-pink charge-transfer ($O_2 \rightarrow Fe$) absorption suggest that the Fe(II)–L^1 complex may serve as a model of hemerythrin. A parallel autoxidation reaction was measured with cobalt(II)–L^1, which also yields a stable brown-colored 2:1 $(CoL^{2+})_2$–O_2 adduct. The oxygenation constant K'_{O_2} ($=[(ML^1)_2O_2]/[ML^1]^2[O_2]$) is a little smaller for iron (8.8×10^7 M^{-2}) than for cobalt (4.4×10^9 M^{-2}). Comparative kinetic studies of the autoxidation of the iron and cobalt complexes showed a common rate law (first order in $[ML^1]$ and also in $[O_2]$), with the second-order rate constant for the iron system (1.4×10^2 M^{-1} s^{-1} at 25 °C) being much smaller than that for the cobalt (3.1×10^4 M^{-1} s^{-1}).

There has been considerable interest in the structure and the properties of metal complexes containing coordinated dioxygen.[2-6] These studies are mostly centered on iron and cobalt complexes, the former being of foremost biological interest and the latter appearing to function as excellent general models for metal–dioxygen binding.

It is now widely accepted that dioxygen reacts with metal chelates ML^{2+} in the following sequence:

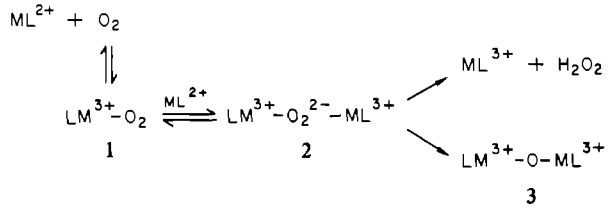

The oxygenated intermediates superoxo (**1**) and μ-peroxo (**2**) species of cobalt chelates are stable enough to permit characterization in the solid state or in solution. Thus the general mechanisms and ligand structural features leading to them are fairly well understood. On the other hand, despite the recent active investigations, the examples of stable O_2 adducts with iron chelates are still very limited. Most of the oxygenated species identified are unstable at normal conditions, and their measurement had to be carried out at low temperature and/or in aprotic solvents. The principal reason is a well-known trend of the rapid irreversible autoxidation to μ-oxo dimers **3** as the ultimate and most favorable products. Collman's "picket-fence porphyrin"[7,8] and Baldwin's "capped porphyrin"[9] are the rare systems that can stabilize the initial intermediate 1:1 O_2 adduct **1** at ambient temperature. The μ-peroxo complex **2** had long been postulated[10-12] and only recently was detected as a transient species at −80 °C with L = porphyrin.[13] The 2:1 O_2 adduct structure is also of interest as an O_2 binding model of hemerythrin, a biological oxygen carrier.[14,15]

No other synthetic or biological ligand ever succeeded in stabilizing the oxygenated intermediates **1** or **2** with iron, except for porphyrin-like macrocyclic polyimines with conjugate double bonds.[16,17] Autoxidation of iron(II) complexes of saturated macrocyclic tetraamine ligands in general proceeds (without detectable formation of an iron–dioxygen complex) to Fe(III)–oxo species in the presence of water or to the oxidative dehydration of the ligands under anhydrous conditions.[18-22] There has been no report of O_2 adduct formation using aliphatic polyamine systems.

Recently we have shown that cobalt(II) complexes of saturated macrocyclic tetra- and pentaamines form stable 1:1[23] and 2:1 O_2 adducts.[24,25] It has been proven that these macrocyclic ligand systems have several advantages and merit further extensive studies in oxygenation: first, they greatly stabilize metal chelates, which shifts the equilibrium $Co^{2+} + L + O_2 \rightleftharpoons (CoL)_nO_2$ in favor of the oxygenation; second, the O_2 adducts are kinetically stabilized, probably because autoxidation to Co^{3+} complexes is prevented due to the difficulty in changing the macrocyclic ligand configurations to accompany the "inner-sphere" electron transfer; third, the macrocyclic chelate structures are under rigid stereochemical control,

(1) (a) Hiroshima University; (b) Hirosaki University; (c) Ehime University.
(2) R. G. Wilkins, *Adv. Chem. Ser.*, No. **100**, 111 (1971).
(3) F. Basolo, B. M. Hoffman, and J. A. Ibers, *Acc. Chem. Res.*, **8**, 384 (1975).
(4) G. McLendon and A. E. Martell, *Coord. Chem. Rev.*, **19**, 1 (1976).
(5) B. R. James, "The Porphyrins", Vol. 5, Part C, D. Dolphin, Ed., Academic Press, New York, 1978, p 205.
(6) R. D. Jones, D. A. Summerville, and F. Basolo, *Chem. Rev.*, **79**, 139 (1979).
(7) J. P. Collman, *Acc. Chem. Res.*, **10**, 265 (1977).
(8) J. P. Collman, R. P. Gagne, C. A. Reed, T. R. Halbert, G. Lang, and W. T. Robinson, *J. Am. Chem. Soc.*, **97**, 1427 (1975).
(9) J. Almog, J. E. Baldwin, and J. Huff, *J. Am. Chem. Soc.*, **97**, 227 (1975).
(10) O. H. W. Kao and J. H. Wang, *Biochemistry*, **4**, 342 (1965).
(11) J. O. Alben, W. H. Fuchman, C. A. Beaudrean, and W. S. Caughey, *Biochemistry*, **7**, 624 (1968).
(12) I. A. Cohen and W. S. Caughey, *Biochemistry*, **7**, 636 (1968).
(13) D. H. Chin, G. N. La Mar, and A. L. Balch, *J. Am. Chem. Soc.*, **102**, 4344 (1980).
(14) I. M. Klotz, G. L. Klippenstein, and W. A. Mendrickson, *Science (Washington, D.C.)*, **192**, 335 (1976).
(15) D. M. Kurz, Jr., D. F. Shriver, and I. M. Klotz, *Coord. Chem. Rev.*, **48**, 951 (1977).
(16) D. Vanderschmitt, K. Bernauer, and S. Fallab, *Helv. Chim. Acta*, **48**, 951 (1965).
(17) J. E. Baldwin and J. Huff, *J. Am. Chem. Soc.*, **95**, 5757 (1973).
(18) J. C. Dabrowiak, F. V. Lovecchio, V. L. Goldken, and D. H. Busch, *J. Am. Chem. Soc.*, **94**, 5502 (1972).
(19) J. C. Dabrowiak, P. H. Merrell, and D. H. Busch, *Inorg. Chem.*, **11**, 1979 (1972).
(20) D. D. Watkins, Jr., D. P. Riley, J. A. Stone, and D. H. Busch, *Inorg. Chem.*, **15**, 387 (1976).
(21) K. D. Hodges, R. G. Wollmann, E. K. Barefield, and D. H. Hendrickson, *Inorg. Chem.*, **16**, 2746 (1977).
(22) V. L. Goedken, P. H. Merrell, and D. H. Busch, *J. Am. Chem. Soc.*, **94**, 3397 (1972).
(23) K. Ishizu, J. Hirai, M. Kodama, and E. Kimura, *Chem. Lett.*, 1045 (1979).
(24) M. Kodama and E. Kimura, *J. Chem. Soc., Dalton Trans.*, 327 (1980).
(25) M. Kodama and E. Kimura, *Inorg. Chem.*, **19**, 1871 (1980).

0020-1669/82/1321-0595$01.25/0

enabling compulsive coordination to permit individual parameterization of equatorial and axial effects; fourth, synthetic strategies by modification of the basic structures are easily achieved; and fifth, they are water soluble, which allows the precise quantitative measurements in aqueous solutions.

Herein we present a new pentadentate ligand, pyridyl-containing 16-membered macrocyclic pentaamine (L^1),[26] that

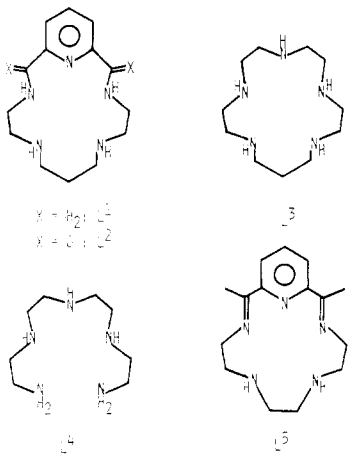

stabilizes a pink-colored dioxygen adduct of iron(II) in aqueous solutions at room temperature prior to a slow degradation to final Fe(III)–oxo products. Saturated macrocyclic pentaamine ligands L^1 and L^3 were expected to form five-coordinate, square-pyramidal iron(II) complexes, probably with high spin, since they would not exert sufficient ligand field strength to cause spin pairing. The high-spin, five-coordinate iron(II) sites are found in deoxymyoglobin and deoxyhemoglobin. This paper reports the equilibrium and kinetics results of the oxygenation of iron(II)–macrocyclic pentaamines in aqueous solutions. The presence of a pyridine ring in the macrocycle is remarkably effective in stabilizing the O_2 adduct, as seen by comparison of the reactions with the L^1 and L^3 systems. The oxygenated intermediate from the Fe(II)–L^3 complex is very short-lived and undergoes much faster autoxidation to the Fe(III)–oxo species. With a similar but unsaturated macrocyclic pentaimine L^5, the red-brown colored iron(III)–μ-oxo complex (FeL)–O–(FeL), where the five nitrogen atoms form the equatorial apices and are coplanar with the iron atom,[27,28] was previously isolated in the autoxidation. For assessment of the (hitherto unknown) equilibrium and kinetics parameters for the Fe(II)–macrocyclic pentaamine system, we also have determined the relevant values for the Co(II)–L^1 system. The values for Co(II)–L^3 were reported earlier.[25]

Experimental Section

For synthesis of the macrocyclic pentaamine L^1, diethyl pyridine-2,6-dicarboxylate was first treated with 3,7-diazanonane-1,9-diamine in refluxing EtOH for 3 days. The concentration of EtOH to ca. $^1/_4$ volume yielded a precipitate, which was purified by recrystallization from EtOH. The product L^2 (mp 202–204 °C; mass spectrum 291 (M^+); IR ν_{CO} 1650 cm^{-1}) was reduced with diborane in THF to get L^1, purified as the HBr salt (recrystallized from AcOH–HBr). Anal. Calcd for $C_{14}H_{25}N_5 \cdot 4HBr$: C, 28.6; H, 5.0; N, 11.9. Found: C, 28.7; H, 5.2; N, 11.7. NMR (in D_2O) δ (external Me_4Si) 2.22 (quint, 2 H), 3.38 (t, 4 H), 3.70–3.90 (m, 8 H), 4.44 (s, 4 H), 7.64 (d, 2 H), and 8.04 (quart., 1 H). The mixed protonation constants log K_i (at I = 0.20 M) were determined potentiometrically: 9.59, 8.67, 5.91, ~2 (at 20 °C); 9.48, 8.56, 5.83, ~2 (at 25 °C); and 9.27, 8.35, 5.68, ~1.8 (at 35 °C). The ligand L^3 was described in a previous paper.[29] Its log K_i (at I = 0.2 M) values used are 10.42, 9.27, 7.06, ~1.7, and ~1.4 at 35 °C. Stock solutions of iron(II) were freshly prepared from analytical grade Mohr's salt ($FeSO_4(NH_4)_2SO_4 \cdot 6H_2O$) and standardized by $KMnO_4$ titration. Iron(II) was free of iron(III): the standard solution with or without treatment of Zn metal consumed the same amount of $KMnO_4$ titrant. Stock solutions of cobalt(II) were prepared from analytical grade $CoCl_2$ and standardized by the method of Schwarzenbach.[30] Potentiometric apparatus, polarographic and cyclovoltammetric apparatus, and general procedures were the same as those used earlier.[24,25,31]

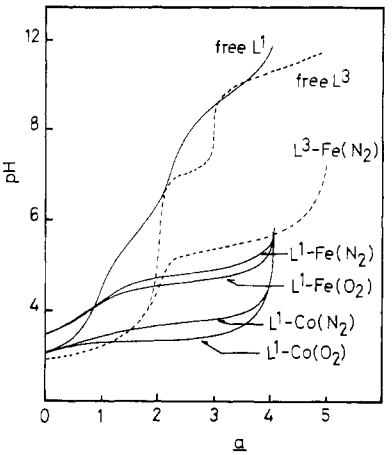

Figure 1. Potentiometric titration of L^1 and L^3 with or without the presence of excess (with L^1) or equimolar (L^3) metal ions in N_2 atmosphere (N_2) and in air (O_2).

Potentiometric Measurements. The ligand hydrobromide salt $L^1 \cdot 4HBr$ or $L^3 \cdot 5HBr$ in 50 mL of aqueous solution (10^{-3} M) was titrated potentiometrically with standard NaOH solution (0.1 M) in the presence of an equimolar amount (only at 20 °C with Fe to lessen the possible Fe hydrolysis) or large excess (10^{-2} M) of Fe^{2+} or Co^{2+}. The $-\log [H^+]$ (=pH) values were recorded after equilibration (2–3 min at each addition of the titrant at 35 °C for both Fe and Co systems). The anaerobic (in N_2) and aerobic complex formation curves were used (see Figure 1) to compute stability constants K_{ML} and oxygenation constants K_{O_2}, respectively. The molar concentration of O_2 in air-saturated aqueous solution was taken from the literature:[32] 3.0×10^{-4}, 2.7×10^{-4}, and 2.3×10^{-4} M at 20, 25, and 35 °C, respectively. Ionic strength was maintained at 0.2 M by addition of $NaClO_4$. Three titrations were performed for each system.

Kinetic Measurements. The rate of O_2 uptake by the Fe^{2+}–L^1 complex (preformed in situ under rigorous anaerobic conditions by mixing Fe^{2+} with 2–3% excess L^1) in Tris buffer was measured with a stopped-flow apparatus by monitoring the increase in absorbance at 540 nm due to the formation of the μ-peroxo complex. The O_2-uptake rate constants were determined either from the second-order plots (unequal concentration) or from the observed pseudo-first-order rate constants.

The rate of O_2 uptake by the Co^{2+}–L^1 complex (prepared also in situ) in the presence of a large excess of L^1 (to minimize the L^1 dissociation) in acetate buffers was measured by following the absorption at 325 nm due to the μ-peroxo complex, and the second-order rate constant was determined by the initial slope method. Three kinetic runs were conducted for all the systems. Typical rate data are given in Tables I and II.

Results

Potentiometric Determination of K_{ML}. The titration of the ligand $L^1 \cdot 4HBr$ showed inflection points at a = 1 and 4 (a is number of moles of base added per mole of ligand) in anaerobic conditions in the presence of large (10 times) excess of metal ion. For the pH-buffer region ($2.40 < a < 3.50$ with Fe, $2.0 < a < 3.50$ with Co) plots of $[\alpha(\alpha_H)_L - \beta_H C_L]$ vs. $(4C_L$

(26) 3,6,10,13,19-Pentaazabicyclo[13.3.1]nonadeca-1(19),15,17-triene.
(27) J. D. Curry and D. H. Busch, *J. Am. Chem. Soc.*, **86**, 592 (1964); S. M. Nelson and D. H. Busch, *Inorg. Chem.*, **8**, 1859 (1969).
(28) E. Fleischer and S. Hawkinson, *J. Am. Chem. Soc.*, **89**, 720 (1967).
(29) M. Kodama and E. Kimura, *J. Chem. Soc., Dalton Trans.*, 104 (1978).
(30) G. Schwarzenbach, "Complexometric Titrations", Interscience, New York, 1957, p 82.
(31) M. Kodama and E. Kimura, *J. Chem. Soc., Dalton Trans.*, 694 (1981).
(32) "Chemical Handbook" ("Kagaku-Binran"), Chemical Society of Japan, Maruzen, Tokyo, 1973, p 571.

$- \alpha$) gave linear lines passing through the origin. This relation fits eq 1 for 1:1 ML^{2+} complex formation, which is a modified form of eq 11 of ref 33 for tetraamine bases instead of triamines.

$$[\alpha(\alpha_H)_L - \beta_H C_L]/[M^{2+}] = K_{ML}(4C_L - \alpha) \quad (1)$$

$$C_L = [L]_{uncomplexed} + [ML^{2+}] \quad (2)$$

$$\alpha = [H^+] + aC_L = 4[ML^{2+}] + 4[L] + 3[HL^+] + 2[H_2L^{2+}] + [H_3L^{3+}] \quad (3)$$

$$(\alpha_H)_L = 1 + [H^+]K_1 + [H^+]^2K_1K_2 + [H^+]^3K_1K_2K_3 + [H^+]^4K_1K_2K_3K_4 \quad (4)$$

$$\beta_H = 4 + 3[H^+]K_1 + 2[H^+]^2K_1K_2 + [H^+]^3K_1K_2K_3 \quad (5)$$

The pH-buffer curve of the anaerobic titration of $L^3 \cdot 5HBr$ in the presence of equimolar Fe^{2+} gave a linear relation between $[\alpha(\alpha_H)_L - \beta_H C_L][5(\alpha_H)_L - \beta_H]$ and $(5C_L - \alpha)^2(\alpha_H)_L$, indicating 1:1 Fe–$L^3$ complex formation, and K_{FeL} was determined from the gradient. An identical procedure was employed to determine K_{CoL} for L^3 (see eq 10 of ref 17). In the calculations, the hydrolysis of $M^{2+}{}_{aq}$ was ignored by considering the small values $10^{3.96}$ (Co) and $10^{4.3}$ (Fe) for K_{OH} ($[M(OH)^+]/[M^{2+}][OH^-]$)[34] and the acidic pH ranges used.

Potentiometric Determination of K_{O_2}. The aerobic titration curves in the presence of excess Fe^{2+} or Co^{2+} (i.e., $C_M \gg C_L$) represent μ-peroxo formation (6). The oxygenation constants

$$2M^{2+} + 2L + O_2 \rightleftharpoons ML\text{–}O_2\text{–}ML$$

$$K_{O_2} = \frac{[ML\text{–}O_2\text{–}ML]}{[M^{2+}]^2[L]^2[O_2]} \quad (6)$$

K_{O_2} can be readily derived as in (7) by appropriate combination of eq 8–10 for $[(ML)_2O_2]$, [L], and $[M^{2+}]$ to substitute into (6). As expected for (7), plots of $[\alpha(\alpha_H)_L - \beta_H C_L]^{1/2}[4(\alpha_H)_L - \beta_H]$ vs. $(4C_L - \alpha)$ gave linear lines passing the origin for the Fe–L^1 and Co–L^1 systems. All the equilibrium constants thus obtained are summarized in Table III.

$$K_{O_2} = \frac{[\alpha(\alpha_H)_L - \beta_H C_L][4(\alpha_H)_L - \beta_H]}{2(4C_L - \alpha)^2 C_M{}^2[O_2]} \quad (7)$$

$$\alpha = [H^+] + aC_L = 4[L] + 3[HL^+] + 2[H_2L^{2+}] + [H_3L^{3+}] + 8[(ML)_2O_2] + [M(OH)^+] \approx 8[(ML)_2O_2] + \beta_H[L] \quad (8)$$

$$C_L = 2[(ML)_2O_2] + [L]_{uncomplexed} = 2[(ML)_2O_2] + (\alpha_H)_L[L] \quad (9)$$

$$C_M \approx [M^{2+}] \quad (10)$$

Polarographic Determination of O_2-Adduct Stoichiometry. The air-saturated control solutions ($[O_2] = 2.7 \times 10^{-4}$ M in 0.10 M acetate buffer, at pH 5.80, $I = 0.2$ M, 25 °C) showed a wave height of 9.70 cm at −0.350 V vs. SCE. Mixing O_2 (1.35×10^{-4} M) with FeL^{2+} (5×10^{-4} M) for a limited time (2 min) lowered the wave height to 4.05 cm. After N_2 bubbling for 30 min (by which time all of the uncoordinated O_2 is completely purged, but the coordinated O_2 remains intact, as concluded from the unchanged visible absorbance due to the O_2 adduct), the solution showed a wave height of 2.65 cm. The concentration of the uncoordinated O_2 corresponds to 4.05 − 2.65 = 1.40 cm in the wave height. The concentration of the O_2 absorbed for O_2-adduct formation is thus $1.35 \times 10^{-4} - ((1.40/9.70) \times 2.7 \times 10^{-4}) = 9.6 \times 10^{-5}$ M. Meanwhile from the optical absorbance of 0.038 and molar absorbance of 187 at 540 nm, the concentration of the O_2 adduct formed is calculated as 2.0×10^{-4} M. Or from the wave height of 6.20 cm after FeL^{2+} (5×10^{-4} M) is 100% converted into the O_2 adduct (exposed to air-saturated solution more than 30 min), the concentration of the O_2 adduct formed when mixed with 1.35×10^{-4} M of O_2 is calculated as $5 \times 10^{-4} \times 2.65/6.20 = 2.1 \times 10^{-4}$ M. Hence the FeL^{2+}:O_2 stoichiometry is (2.0 (or 2.1) $\times 10^{-4}$):$(9.6 \times 10^{-5}) \approx 2:1$. A similar experiment in 0.1 M Tris buffer (pH 8.30) also established the 2.0:1 stoichiometry.

The 2:1 stoichiometry was also found for the Co^{2+}–L^1 system with the identical method as described for Co^{2+}–L^3 previously.[25]

Electrochemical Behavior of Iron(II)–L^1 and –L^3. Both iron(II)–L^1 and –L^3 macrocyclic complexes underwent one fairly reversible oxidation producing iron(III) species in Tris buffers. Figure 2 shows a typical current–voltage response for the iron(II)–L^1 complex. The separation of anodic and cathodic peaks ΔE was ~200 mV (the theoretical ΔE for a completely reversible system is 59.5 mV for a one-electron exchange) for both systems, and peak height ratios were nearly unity. Slight variations (±3 mV) of peak potential separation with different scan rates (20–300 mV s^{-1}) were observed. Both peak heights were proportional to the square root of the scan

Table I. Kinetic Data for Iron-μ-Peroxo Complex $(FeL^1)_2O_2$ Formation[a]

$10^3 \times [FeL^{2+}]$, M	$10^3 \times [O_2]$, M	pH	$10^{-2}k_1$, M^{-1} s^{-1}	k_{obsd},[b] s^{-1}
1.00	0.135	8.59	3.3_4	
0.50	0.135	8.59	3.3_0	
0.25	0.135	8.59	3.4_5	
1.00	0.067_5	8.59	3.2_1	
1.00	0.033_8	8.59	3.6_0	
1.00	0.135	9.50	6.9_4	
1.00	0.135	9.02	5.1_5	
1.00	0.135	8.27	2.1_6	
1.00	0.135	8.00	1.4_0	
6.0	0.135	8.80		2.4_0
3.0	0.135	8.80		1.2_2
2.0	0.135	8.80		0.79_3
1.0	0.135	8.80		0.40
0.75	0.135	8.80		0.30
0.60	0.135	8.80		0.23_5
0.50	0.135	8.80		0.19_1
0.375	0.135	8.80		0.14
0.188	0.135	8.80		0.067

[a] [Tris] = 5×10^{-2} M. [b] See eq 18.

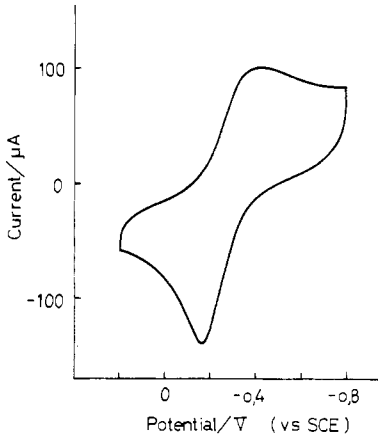

Figure 2. Cyclic voltammogram of $(FeL^1)^{2+}$ (10^{-3} M) in Tris buffer (0.05 M) at a glassy carbon electrode ($E^\circ = -0.7$ V vs. SCE, pH 9.25, $I = 0.2$ M ($NaClO_4$), scan rate = 100 mV s^{-1}, and at 25 °C).

(33) M. Kodama and E. Kimura, *J. Chem. Soc., Dalton Trans.*, 1081 (1978).
(34) J. A. Bolzen and A. J. Aruia, *Electrochim. Acta*, 7, 589 (1962).

Table II. Kinetic Data for Cobalt-μ-Peroxo Complex $(CoL^1)_2O_2$ Formation

$10^3[CoL^{2+}]$, M	$10^3[O_2]$, M	$10^3[L^1]$, uncomplexed, M	$[OAc^-]$, M	pH	initial slope, M s^{-1}	$10^{-4}k$, M^{-1} s^{-1}
0.50	0.135	1.0	100	5.60	$2.0_3 \times 10^{-3}$	3.0_0
0.50	0.135	1.0	100	5.20	$2.1_0 \times 10^{-3}$	3.1_1
0.50	0.135	1.0	100	4.50	$2.0_0 \times 10^{-3}$	2.9_6
0.25	0.135	1.0	100	5.20	$1.1_0 \times 10^{-3}$	3.2_6
0.50	0.067_5	1.0	100	5.20	$1.0_0 \times 10^{-3}$	3.2_0
0.25_0	0.067_5	1.0	100	5.20	$5.1_0 \times 10^{-4}$	3.2_6
0.50	0.135	1.0	100	5.20	$2.0_3 \times 10^{-3}$	3.0_0
0.50	0.135	1.0	50	5.20	$1.9_5 \times 10^{-3}$	2.8_9
0.50	0.135	3.0	100	5.20	$2.2_0 \times 10^{-3}$	3.2_6
1.00	0.135	1.0	100	5.20	$4.0_0 \times 10^{-3}$	3.0
2.50	0.135	1.0	100	5.20	$1.0_5 \times 10^{-2}$	3.1

Table III. Comparison of Equilibrium Constants (with Confidence Limits) for ML^{2+} Complexation and O_2-Adduct $(ML)_2O_2$ Formation at 35 °C and $I = 0.2$ M Unless Otherwise Listed

metal	ligand	K_{ML}	K_{O_2} [a]	K'_{O_2} [b]
Fe	L^1	$(5.8 \pm 0.9) \times 10^{10}$	$(3.0 \pm 0.5) \times 10^{29}$	8.8×10^7
	L^3	$(3.7 \pm 0.8) \times 10^{14}$		
	L^4 [c]	$10^{9.85}$		
Co	L^1	$(9.1 \pm 1.0) \times 10^{13}$	$(3.6 \pm 0.5) \times 10^{37}$	4.4×10^9
	L^3 [d]	$10^{16.0}$	$10^{39.7}$	$10^{7.9}$
	L^4 [e]	$10^{13.7}$	$10^{43.2}$	$10^{15.8}$
	L^6 [e]	$10^{14.0}$	$10^{42.6}$	$10^{14.7}$

[a] Defined by eq 6. [b] $K'_{O_2} = K_{O_2}/(K_{ML})^2$. [c] Reference 37. At 25 °C and $I = 0.1$ M (KCl). [d] Reference 25. [e] Reference 36. At 25 °C and $I = 0.1$ M (KCl).

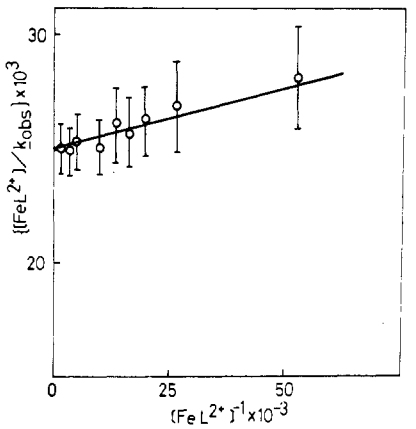

Figure 3. Plot (with confidence limits) of eq 19 in the text for Fe–L^1.

rate. These facts are indicative of quasi-reversible (one-electron)[35] electrochemical behavior, and therefore the midpoint between two peaks is a reasonable estimate of the electrode potential corresponding to the polarographic half-wave potential. Thus determined oxidation potentials are

$$E^{\phi}_{oxid}(Fe\text{–}L^1) = -0.27 \text{ V vs. SCE}$$

$$E^{\phi}_{oxid}(Fe\text{–}L^3) = -0.04 \text{ V vs. SCE}$$

These values are independent of the solution pH range (8.0–9.5) and the concentration of the complexes (10^{-2}–10^{-3} M) or of excess ligands (10^{-2}–10^{-3} M).

Kinetics of Peroxo Complex Formation. Cobalt. The rates were first order in $[CoL^{2+}]$ and in $[O_2]$. The second-order rate constants were independent of acetate buffer concentrations, and 4.50 < pH < 5.60 (where the oxygenation occurs, as indicated by the pH titration curve; see Figure 1).

Iron. The kinetics were measured in Tris buffers (8.0 < pH < 9.5) where practically no dissociation of the Fe^{2+}–L^1 complex would occur: the calculated degree of dissociation at pH 8.25 is 2.0×10^{-4} for $[FeL^1] = 10^{-3}$ M. At a given pH the reaction was first order in $[FeL^1]$ and in $[O_2]$. The second-order rate constants k significantly varied with pH, which was resolved in terms of the two simultaneous reactions

$$FeL^1 + O_2 \xrightarrow[FeL^1]{k_O} (FeL^1)_2O_2 \quad (11)$$

$$FeL^1(OH) + O_2 \xrightarrow[FeL^1]{k_{OH}} (FeL^1)_2O_2 + OH^- \quad (12)$$

The net rate constant k is then expressed by

$$k = \frac{k_O + k_{OH}K^{OH}[OH^-]}{1 + K^{OH}[OH^-]} \quad (13)$$

where

$$K^{OH} = \frac{[FeL^1(OH^-)]}{[FeL^1][OH^-]} \quad (14)$$

If we assume $k >> k_O$, then (13) can be approximated to (15),

$$k = \frac{k_{OH}K^{OH}[OH^-]}{1 + K^{OH}[OH^-]} \quad (15)$$

$$k^{-1} = \frac{1}{k_{OH}} + \frac{1}{k_{OH}K^{OH}[OH^-]} \quad (16)$$

which is rearranged to (16). Plots of k^{-1} vs. $[OH^-]$ gave a linear line with a finite intercept. From the intercept k_{OH} is estimated as 7.4×10^2 M^{-1} s^{-1}. K^{OH} ($=1.3 \times 10^5$ M^{-1}) is determined from intercept/slope.

More elaborately, consider reaction 17. Assuming a steady

$$FeL^{2+} + O_2 \underset{k_{-1}}{\overset{k_1}{\rightleftharpoons}} (FeL)O_2^{2+} \underset{k_{-2}}{\overset{+FeL^{2+}\ k_2}{\rightleftharpoons}} (FeL)_2O_2 \quad (17)$$

$$\text{rate} = \frac{k_1k_2[FeL^{2+}]^2[O_2]}{k_{-1} + k_2[FeL^{2+}]} = k_{obsd}[O_2] \quad (18)$$

state of $(FeL)O_2$ and using the initial rate data where the term $k_{-2}[(FeL)_2O_2]$ is small, one obtains eq 18 (where k_{obsd} is the pseudo-first-order rate constant; see Table I). Inverting (18) leads to

$$\frac{[FeL^{2+}]}{k_{obsd}} = \frac{k_{-1}}{k_1k_2}\frac{1}{[FeL^{2+}]} + \frac{1}{k_1} \quad (19)$$

A plot of $[FeL^{2+}]/k_{obsd}$ vs. $[FeL^{2+}]^-$ (at constant $[O_2]$) is shown in Figure 3. The linearity required for mechanism 17 is satisfied. The plot also confirms that within confidence limits, the reaction is first order in $[FeL^{2+}]$, as so established

(35) One-electron oxidation for the Fe–L^1 system was further established from the anodic polarographic wave height of 6.1 cm for the Fe(II)–L^1 complex (0.80 mM in Tris buffer, pH 8.5, $I = 0.2$ M), which is half the height of 11.5 cm for the two-electron oxidation wave of $Hg + L^1 \xrightarrow{-2e} (HgL^1)^{2+}$, i.e., mercury dissolution wave due to L^1 (0.08 mM in the same buffer).

Table IV. Rate Constants (with Confidence Limits All in M^{-1} s^{-1}) for the Formation of μ-Peroxo Complexes $(ML)_2O_2$ at 25 °C and I 0.2 M

M	L	k^a
Fe	L^1	$(1.4 \pm 0.2) \times 10^2$ [b]
Co	L^1	$(3.1 \pm 0.5) \times 10^4$
	L^3	2.2×10^5 [c]
	L^4	$\sim 10^5$ [d]

[a] The second-order rate constants for the reaction between ML^{2+} and O_2. [b] At pH 8.0. [c] Reference 25. [d] Reference 54.

by the second-order log-plot treatment. The oxygenation rate constants for the present and relevant systems are summarized in Table IV.

Discussion

Characterization of the M(II) Complexes in Aqueous Solutions. To our knowledge, this is the first report on L^1. Comparison with the linear analogue L^6 described earlier[36]

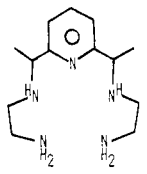

L^6

is helpful in understanding the chemical properties of the macrocyclic ligand. Like L^6, L^1 behaves as a tetraamine base and is isolated as the HBr salt. Obviously it is the four aliphatic amines that are protonated, as was considered for L^6.[36] The protonation constants log K_i for L^1 (9.48, 8.56, 5.83, and ~2 at 25 °C, I = 0.2 M) are generally in a similar range with the corresponding values for L^6 (9.75, 9.05, 6.32, and 5.47).[36] The exceptionally low value of log K_4 for L^1 (cf. the log K_4 value for L^6) means very few of the nitrogen lone pairs are available for the fourth protonation, with three protons already congesting the polyamine macrocyclic cavity. A similar phenomenon was seen with the aliphatic system: compare macrocyclic L^3 (log K_i = 10.64, 9.49, 7.28, ~1.7, ~1.5)[29] and linear L^4 (log K_i = 9.85, 9.27, 8.19, 5.08, 3.43).[37]

The anaerobic pH titrations of the L^1–Fe(II), L^3–Fe(II), and L^1–Co(II) systems all gave simple curves like those found at 1:1 Fe(II)–L^4 [37] and Co(II)–L^3 interactions.[25] There was little sign of oxidation of the metal ion (e.g., color change or precipitation) during the titrations. All of the complexation equilibria fit only eq 1, precluding chelate protonation (to form MHL^{3+}, etc.) or hydrolysis (to $M(OH)L^+$, etc.). Thus, we have determined the formation constants for the 1:1 M(II)–macrocyclic polyamine complexes as before.[25]

It is significant to find that the macrocyclic pentaamines tend to sequester iron(II) from ready oxidation and hydrolysis in aqueous solutions, a property unparalleled with linear pentaamine homologues or lower polyamine macrocycles. Under the rigid stereochemical control the macrocyclic pentaamines would most effectively adopt square-pyramidal, five-coordinate configurations.[38] The contribution of the extra, fifth N donor atom to both thermodynamic and kinetic stabilization of Fe(II)–macrocyclic polyamine complexes was proved when a 14-membered tetraamine homologue "cyclam"–Fe(II) was titrated under the same conditions: no sooner had the Fe(II)–cyclam complexation started (at $a \approx 2$) than brown precipitation of Fe(III)–oxo species occurred (at $a \approx 2.5$, pH 7–8); i.e., the Fe(II)–cyclam complex is much more air sensitive.[39]

As occurred for Co(II),[25] Cu(II),[29] Zn(II), etc.,[33] the cyclization of linear L^4 (log $K_{FeL} \approx 10$)[37] into 16-membered macrocyclic L^3 (log K_{FeL} = 14.6) enhances the thermodynamic stability of the complex with Fe(II): log K_{FeL} of L^4 at 35 °C was estimated on the basis of the reported values for ΔH (=−8.7 kcal/mol) and ΔS (=16.0 eu).[37] The greater complexing ability of L^3 with respect to that of quinquedentate L^4 is compatible with the presence of five coordinating bonds in the L^3 complex. With the pyridyl-containing counterparts, the cyclization does not seem to raise the complex stability, as shown by comparison of log K_{CoL} values for L^1 (14.0) and L^6 (16.0).[36,40] A molecular model of L^1 indicates that the pyridine ring would stay on the equatorial plane. The greater steric strain involved at the coordination of the pyridine ring in the constrained macrocyclic configuration may work unfavorably for the L^1 complexation.

The general complex stability trend with linear polyamines[41] is also obeyed with the macrocyclic systems L^1 and L^3, which form more stable complexes with Co(II) than with Fe(II).

The macrocyclic pentaamine complexes of Fe(II) in aqueous solutions exhibited cyclic voltammograms indicating a one-electron process in a fairly reversible manner electrochemically, which is a reflection of the characteristic stabilization (in both the thermodynamic and kinetic sense) of the macrocyclic pentaamine complexes at the metal redox processes. This is the first report of cyclic voltammetry of Fe–polyamine complexes measured in aqueous solutions. Earlier measurements[18,42,43] were all performed in aprotic solvents. The remarkable potential of the macrocyclic polyamine ligands was previously demonstrated in the stabilization of unusual oxidation states of Ni(III) and Cu(III) in aqueous solutions by the fairly reversible cyclic voltammograms for Cu(II)/Cu(III) and Ni(II)/Ni(III) couples.[31,44] Another interesting finding is the relatively low redox potentials for Fe(II)–L^1 (−0.02 V vs. NHE) and Fe(II)–L^3 (+0.21 V), which lie within the range of those for biological hemin complexes,[45] e.g., hemoglobin (~+0.2 V, at pH 7) and turnip peroxidase (~−0.25 V). These features about the five-coordinate Fe(II)–macrocyclic pentaamine complexes suggest their potential as models of O_2 uptake or redox biological molecules.

The iron(II)–macrocyclic pentaamine complexes may also serve as synthetic analogues for the active site of the anticancer agent bleomycin (BLM).[46] The biologically active form of

(36) W. R. Harris, I. Murase, J. H. Timmons, and A. E. Martell, *Inorg. Chem.*, **17**, 889 (1978).
(37) P. Paoletti and A. Vacca, *J. Chem. Soc.*, 5051 (1964).
(38) We could not detect an ESR signal for the Fe(II)–L^1 complex maintained at liquid-nitrogen temperature in anaerobic conditions. This fact is not incompatible with an anticipated high-spin state of the Fe(II) complex having a short spin–lattice time. The high-spin, five-coordinated square-pyramidal bleomycin–Fe(II) complex described below is also ESR silent.[46] With the Co(II)–L^1 complex, we failed so far to obtain a distinct ESR spectrum to establish the low-spin state for Co(II). The bleomycin–Co(II) complex is reported to be in the low-spin state.[46]
(39) We very roughly estimate log $K_{FeL} \approx 9$ for the cyclam complex on the basis of the titration data barely obtained from the data before precipitation. The low-spin Fe(II)–cyclam complexes were isolated only from nonaqueous (e.g., acetonitrile) solutions, in which the N_4 forms a square-planar geometry.[20]
(40) This is also true for Cu(II)–L^1 (18.8 at 25 °C and I = 0.2 M; unpublished data) vs. Cu(II)–L^6 (21.2)[31] and for Ni(II)–L^1 (15.2 at 35 °C and I = 0.2 M; unpublished data).
(41) D. L. Wright, J. H. Holloway, and C. N. Reilly, *Anal. Chem.*, **37**, 884 (1965).
(42) M. M. Bishop, J. Lewis, T. D. O'Donoghue, R. R. Raithby, and J. N. Ramsden, *J. Chem. Soc., Dalton Trans.*, 1390 (1980).
(43) S. Koch, R. H. Holm, and R. B. Frankel, *J. Am. Chem. Soc.*, **97**, 6714 (1975).
(44) For instance: D. C. Olson and J. Vasilevskis, *Inorg. Chem.*, **8**, 1611 (1969); **10**, 463 (1971); F. V. Lorecchio, E. S. Gore, and D. H. Busch, *J. Am. Chem. Soc.*, **96**, 3109 (1974); E. Zeigerson, G. Ginzburg, N. Schwartz, Z. Luz, and D. Meyerstein, *J. Chem. Soc., Chem. Commun.*, 241 (1979), and also ref 31.
(45) J. M. Pratt in "Techniques and Topics in Bioinorganic Chemistry", C. A. McAuliffe, Ed., Macmillan, London, 1975, p 148, and references therein.

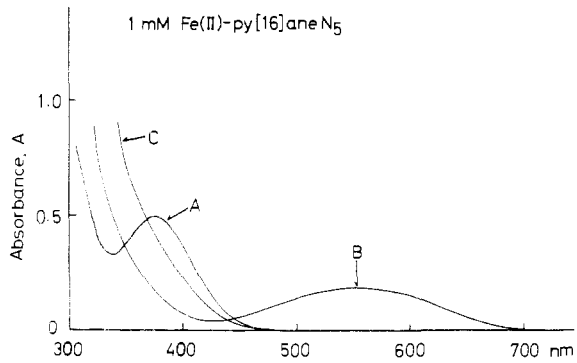

Figure 4. Electronic absorption spectrum in the visible region of (A) Fe(II)–L^1 in degassed Tris buffer at 10^{-3} M, (B) solution A after oxygenation with absorption of 0.5 mol of O_2/mol of Fe, and (C) solution B after 5 h in air.

BLM surrounds iron(II) with five-coordinate pentaamines composed of an amine, pyrimidine N, deprotonated peptide N of histidine residue, and histidine imidazole N as planar (equatorial) ligand donors and an α-amino N as axial donor. It is proposed that the 1:1 BLM–Fe(II) complex having a high-spin square-pyramidal geometry incorporates a dioxygen molecule into the vacant sixth coordination site. The BLM–Fe(II) complex gives a reversible cyclic voltammogram with a low redox potential of 0.165 V.[46] The BLM–Fe(II) complex tends to be oxidized to BLM–Fe(III) via the oxygenated intermediate BLM–Fe^{II}·O_2, whereby superoxide and hydroxyl radicals are efficiently produced. These activated oxygen species attack to cleave DNA bases of cancer cells in the vicinity. Thus, the oxygenation of the macrocyclic pentaamine complexes drew our interest.

Reactivity of the M(II)–L Complexes with Dioxygen in Aqueous Solutions. Upon exposure to air, the light yellow solution of the Fe(II)–L^3 complex turned red-purple, which immediately faded to a colorless solution with occasional brown precipitates (probably of decomposed Fe(III)–oxo species). A similar appearance and a rapid disappearance of violet color were reported with Fe(II)–[14]diene N_4 (14-membered macrocyclic N_4 including two imines) in aqueous solutions.[22] By contrast, a red-purple solution [λ_{max} 540 nm (ϵ 187)] resulting from oxygenation of the yellow Fe(II)–L^1 remained fairly stable at room temperature for ~3 h before its slow degradation to a colorless solution (see Figure 4).

The polarographic measurements have verified the O_2 uptake by the Fe(II)–L^1 complex in aqueous solution to be stoichiometric and reproducible from sample to sample in acetate (pH ~6) and Tris (pH ~8) buffers. In the course of the O_2 uptake, the ligand L^1 remained intact (i.e., we could not detect oxidized or dehydrogenated forms of the ligand), and hydrogen peroxide, a possible product of O_2, was not formed. Further, as confirmed by a separate reaction of Fe(III) with L^1, the red-purple species was not derived from an Fe(III) complex with L^1. On the basis of these pieces of indirect evidence, we propose the purple intermediate observed in the oxygenation of the iron(II)–L^1 complex to be a μ-dioxygen-bridged iron species (FeL)–O_2–(FeL) (see Figure 5) and assign the purple absorption to O_2^{2-} → Fe(III) CT bands. It is pertinent to note that a similar band (490 nm) due to O_2^{2-} → Fe(III) CT energy is reported for the [$Fe^{III}(H_2O)_5O_2^{2-}$] model complex.[47]

In a parallel study with the Co(II)–L^1 complex, the O_2 uptake is also accompanied by intensifying O_2^{2-} → Co(III) CT absorption of golden brown color at 325 nm (ϵ 6250), in

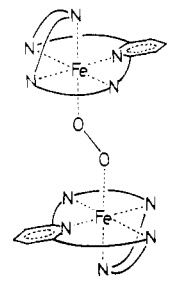

Figure 5. Proposed structure for $(FeL^1)_2O_2$.

common with a number of μ-peroxo cobalt polyamine complexes (CoL)–O_2–(CoL) in the literature.[4] The present polarographic study firmly established the O_2:Co stoichiometry as 1:2, supporting the spectrophotometric results. A similar brown [λ_{max} 320 nm (ϵ 6400)] μ-peroxo complex formation was earlier reported with Co(II)–L^3 complex.[25]

A further analogy can be drawn from the situation proposed to exist for oxyhemerythrin.[14,15] Hemerythrin, an iron(II)-containing O_2 carrier, takes up O_2 with a 2:1 Fe:O_2 stoichiometry to convert the yellow-colored (high-spin) iron(II) atoms into violet-pink (high-spin) iron(III) [λ_{max} 500 nm (ϵ 140/$(Fe)_2O_2$ site)] in oxyhemerythrin having the μ-peroxo bridging structure. The violet absorption band was interpreted as due to a CT process from O_2^{2-} to Fe(III).[47-49]

In the potentiometric titration curves (Figure 1), the pH of the buffer region measured in air is below that of the Fe(II)–L^1 curve under N_2, implying much stronger competition by the metal for the ligand in the metal–dioxygen complex than in the simple Fe(II)–L^1 complex. This observation is most easily explained by considering the effect of partial transfer of an electron from iron to dioxygen, which conforms to the above conclusion that the complex contains binegative O_2^{2-} coordinated to Fe(III). An identical manner of pH lowering at formation of the dioxygen complex was recorded for the Co(II)–L^1 system. Thus the pH curves for Fe and Co were treated by the identical equilibrium (6) to yield the common stability constants K_{O_2} of the oxygen complexes. The reproducible fitness of the theoretical equation (7) to the experimental data at $2 < a < 3.5$ for both Fe and Co is in agreement with the formation of the μ-dioxygen complexes $(ML)^{3+}$–O_2^{2-}–$(ML)^{3+}$. As a correction for metal chelate stabilities, the stability constant K_{O_2} may be recast into a more convenient format, K'_{O_2}, expressed by

$$K'_{O_2} = \frac{[(ML)_2O_2]}{[ML]^2[O_2]} = \frac{K_{O_2}}{K_{ML}{}^2} \qquad (20)$$

Comparison of the K'_{O_2} values (see Table III) reveals that the Fe(II)–L^1 complex possesses a slightly weaker O_2 affinity than the Co(II) counterpart. This is the first comparative data for dioxygen complexes with Fe(II)– and Co(II)–polyamine chelates, and hence until more data are available, we reserve the assessment of the present result. Meanwhile, the effects of Fe(II) and Co(II) as central metal ions on 1:1 O_2 binding are documented with biological systems and porphyrin systems.[4-6,50] The oxygen affinities are in general 10–100 times

(46) Y. Sugiura, *J. Am. Chem. Soc.*, **102**, 5208, 5216 (1980), and references therein.
(47) S. Keresztes-Nagy and I. M. Klotz, *Biochemistry*, **4**, 919 (1965).
(48) K. Garbett, D. W. Parnall, I. M. Klotz, and R. J. P. Williams, *Arch. Biochem. Biophys.*, **103**, 419 (1969).
(49) In the course of oxygenation of the five-coordinate iron(II) complexes Fe(Salen)(py) in the solid state, purple color was observed before the final orange μ-oxo complexes $[Fe(Salen)]_2O$ were formed: R. N. Niswander and A. E. Martell, *Inorg. Chem.*, **17**, 2341 (1978). It is very likely that the purple species are the μ-peroxo intermediates. In fact Niswander and Martell regarded the five-coordinate Salen complexes as a hemerythrin model.
(50) J. P. Collman, J. I. Brauman, K. M. Doxsee, T. R. Halbert, S. E. Hayes, and K. S. Suslick, *J. Am. Chem. Soc.*, **100**, 2761 (1978); J. P. Collman, J. I. Brauman, E. Rose, and K. S. Suslick, *Proc. Natl. Acad. Sci. U.S.A.*, **75**, 1052 (1978).

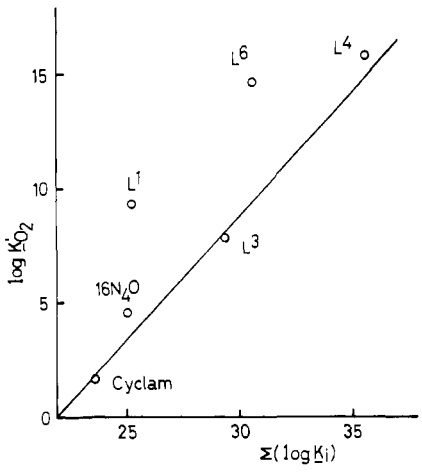

Figure 6. Correlation of log K'_{O_2} (see eq 20) for the Co(II) system with the sum of the log of the protonation constants of the ligands, L^1, L^3 (ref 25), L^4 (ref 36), L^6 (ref 37), cyclam (ref 24), and a 16-membered oxatetraamine abbreviated as $16N_4O$ (ref 25).

greater for Fe than for Co in these systems.

The inclusion of a pyridine ring into the macrocyclic pentaamines adds special electronic and steric effects to oxygenation of the metal complexes. As the cyclic voltammograms indicated, the oxidation of Fe(II) becomes more favorable by the presence of pyridine. There commonly is a linear correlation between the oxygen affinity and the ease of $M^{II \rightarrow III}$ represented by the oxidation potentials,[3] which leads to a suggestion that Fe–L^1 may have a higher tendency to form a dioxygen complex than Fe–L^3. It is unfortunate that we cannot examine this postulate, since the apparently formed dioxygen complex with L^3 (as judged by the purple color) immediately decomposes, to preclude the estimation of its stability constant. The more rigid configuration of L^1 (with respect to L^3) in the μ-peroxo complex may serve to thwart the ligand dissociation and to make the complex kinetically inert. It may be relevant to note that Co–L^1 has a higher K'_{O_2} value than Co–L^3, although we could not find the electrochemical support: the $E_{1/2}$ of the anodic wave corresponding to Co(II)–L^3 → Co(III)–L^3 from polarography was −0.30 V (vs. SCE), while the $E_{1/2}$ value for Co(II)–L^1 was undetermined due to the obscured anodic wave merging with a background wave.

For a series of μ-peroxo cobalt complexes of polyamines including L^1, L^3, L^4, L^6, cyclam, etc., the plot of log K'_{O_2} vs. $\sum \log K_i$ gives a linear line (see Figure 6). A similar linear relation has been established for μ-peroxo-μ-hydroxo cobalt complexes.[4] This is interpreted that as the polyamine ligand basicity increases, its σ-electron donating ability increases, resulting in higher electron density at the metal ion to facilitate the electron transfer to a π^* orbital of molecular oxygen, thus forming a complex. However, the points representing pyridyl-containing ligands L^1 and L^6 lie above the line formed by the aliphatic ligands, indicating abnormally higher affinity for O_2 relative to affinity for protons. An additional effect of the π character of these ligands must be invoked to explain such an anomalous behavior. It should be recalled that with Co(II)–cyclam complexes trans axial ligands (occupying the fifth coordinate site) such as pyridine or NH_3 can stabilize μ-dioxygen complexes mainly by σ donation.[51]

Unlike oxyhemerythrin,[14,15] the sandwiched dioxygens in both oxygenated Fe–L^1 and Co–L^1 complexes are very firmly attached. We could not purge them by mere bubbling N_2 (for 20 min at room temperature) through their aqueous solutions, as concluded by little change of absorptions at 540 nm (with Fe–L^1) and 325 nm (with Co–L^1). A similarly strong O_2 binding was reported for the Co–L^3 system.[25] Hence these macrocyclic pentaamine complexes are devoid of the reversible O_2 uptake capacity.

While structurally mimicking the oxygenated active site of hemerythrin, the present macrocyclic pentaamine complexes do not serve as a model for the anticipated active center of bleomycin, for which uptake of oxygen molecules in monomeric adduct structure is requisite (for the subsequent activation of the O_2); the 1:1 O_2 adduct was actually identified by using Co(II)–BLM.[46] However, as it was shown recently[52] that the incorporation of substituents into dioxocyclam[23] renders the oxygenation products of cobalt complexes (CoL)–O_2–(CoL) into (CoL)–O_2, an appropriate chemical modification of the macrocyclic pentaamines may lead to discovery of better model compounds for the BLM–O_2 interaction and to enlightenment as to the special requirements for Fe to function as an O_2-activating center.[53]

Kinetics of Oxygenation. There have been number of kinetic reports on μ-peroxo complex formation with Co(II) chelates.[4-6] The established mechanism regardless of the chelates is outlined as

$$ML + O_2 \underset{k_{-1}}{\overset{k_1}{\rightleftharpoons}} ML\text{–}O_2 \qquad (21)$$

$$ML\text{–}O_2 + ML \underset{k_{-2}}{\overset{k_2}{\rightleftharpoons}} ML\text{–}O_2\text{–}ML \qquad (22)$$

Under the conditions $[ML] \gg [O_2]$, the rate law for the μ-peroxo complex formation is expressed as $d[\mu\text{-peroxo}]/dt = k_1[ML][O_2]$. This reaction scheme fits the present oxygenated Co–L^1, just as it does other polyamine complexes including Co–L^3,[25] Co–cyclam,[24] and Co–L^4.[54] The second-order rate constant $k_1 = 3.1 \times 10^4\ M^{-1}\ s^{-1}$ is within a normal range (10^4–$10^5\ M^{-1}\ s^{-1}$) for cobalt complexes of various kinds of polyamines,[6] which is accounted for by the explanation[2] that all of these reactions involve the same process of coordinated water replacement by dioxygen, which is dominated by water exchange.

An identical rate law was discovered for the oxygenation of the Fe(II)–L^1 complex under the conditions employed. To our knowledge *this is the first successful kinetic measurement of an iron(II) complex of a nonporphyrin ligand in aqueous solutions.* In autoxidation of an iron(II)–porphyrin or a heme moiety, the kinetics follow first-order dependence both in [Fe–heme] and in $[O_2]$ in some cases[10] and in another case follow second-order dependence in [Fe–heme] and first-order dependence in $[O_2]$.[11,12] The present study further offers the first comparative data for oxygenation of iron(II) and cobalt(II) complexes under the same conditions.

It is established in porphyrin systems[5] and would be applicable to the present macrocyclic pentaamine system that iron(II) with d^6 electronic configuration tends to be six-coordinate while cobalt(II) with d^7 configuration tends to be five-coordinate. Hence, the dissociation of the sixth coordinated molecule (=water in the aqueous solutions) would be more difficult and slower from iron than from cobalt. Provided that this water dissociation is slower than the subsequent O_2 attack, this explanation could account for the smaller rate

(51) G. McLendon and M. Mason, *Inorg. Chem.*, 17, 362 (1978).

(52) R. Machida, M. Kodama, and E. Kimura, manuscript in preparation.

(53) Polarographically we detected H_2O_2 generated from the solution of $(FeL^1)_2O_2$ upon standing. We also observed that $(FeL^1)_2O_2$ oxidizes ascorbic acid and KI. The purple $(FeL^1)_2O_2$ complex (at pH 9 and −196 °C) showed ESR absorptions at $g = 7.04$, 5.58, and 4.27, which are assigned to high-spin octahedral ferric ion. The brown $(CoL^1)_2O_2$ complex failed to show ESR absorptions. The detailed ESR study and resonance Raman studies are in progress to test the appropriateness of viewing the μ-dioxygen center as μ-peroxo.

(54) F. Miller, J. Simplicio, and R. G. Wilkins, *J. Am. Chem. Soc.*, **91**, 1962 (1969).

constant for Fe-L^1 with respect to the one for Co-L^1. With more information on the structures of M(II)-L^1 and $(ML)_2O_2$ (with metal spin states), further rationalization may be invoked. It is of interest to note that myoglobin (Fe-containing) and coboglobin (Co-containing) take up molecular oxygen with almost the same second-order rate constants ($\sim 10^7$ M^{-1} s^{-1}).[5] This fact is consistent with the structural features around metal ions: the iron and cobalt atoms in deoxymyoglobin and deoxycoboglobin, respectively, are both five-coordinate and the oxygen binding sites are both vacant.

The O_2-uptake rate constant with Fe(II)-L^1 varied with pH. Our analysis indicated that the hydroxo species FeL(OH) is a reactive form. Though there is no experimental proof, we tentatively visualize a deprotonated species $FeH_{-1}L$ as an equivalent to the hydroxo species. Deprotonation of the axial amine to a conjugate imide anion may trigger the dissociation of the trans H_2O molecule.

In contrast to the stability constants, the second-order rate constant is about an order smaller for Co(II)-L^1 with respect to that for Co(II)-L^3. This may reflect a weaker σ donation of the pyridyl-containing ligand L^1, which works unfavorably for the water dissociation prior to the O_2 attack.

Detailed characterizations of the oxygenated complexes with variously sized macrocyclic pentaamines are in progress to clarify the structure and mechanism of the interaction between O_2 and the intrinsic Fe(II) chelates, and moreover to correlate them with the mechanisms of the biological O_2-uptake systems such as hemerythrin. Structural modification of the macrocyclic pentaamines may not only give a deeper insight into the oxygenation mechanisms but also produce new synthetic O_2 carriers and possibly O_2-activating enzyme models.

Acknowledgment. We wish to thank the Minister of Education, Japan, for a grant-in-aid for Special Project Research No. 521322.

Registry No. $FeL^{1\,2+}$, 79802-93-0; $CdL^{1\,2+}$, 79802-94-1; $FeL^{3\,2+}$, 79802-95-2; $(FeL^1)_2O_2$, 79802-96-3; $(CoL^1)_2O_2$, 79802-97-4; O_2, 7782-44-7; L^1·4HBr, 79802-91-8; L^2, 79802-92-9; diethyl pyridine-2,6-dicarboxylate, 15658-60-3; 3,7-diazanonane-1,9-diamine, 4741-99-5; L^3, 29783-72-0.

Contribution from the Istituto di Chimica Analitica, University of Turin, 10125 Turin, Italy, and the Istituto di Chimica Analitica ed Elettrochimica, University of Pisa, 56100 Pisa, Italy

Mechanism of Complex Formation: Equilibria and Kinetics of Fe^{3+} and $FeOH^{2+}$ Interactions with Substituted Salicylic Acids

EDOARDO MENTASTI,* FERNANDO SECCO, and MARCELLA VENTURINI

Received January 27, 1981

The kinetics and mechanism of complex formation of reactions between Fe(III) and a series of substituted salicylic acids have been investigated with a stopped-flow technique at μ = 1.0 M ($NaClO_4$) and 25.0 °C. The reactions involve the formation of a 1:1 chelate species, at $[HClO_4] \geq 0.010$ M, with release of protons from both phenolic and carboxylic groups, and the equilibrium quotients of the reactions $Fe^{3+} + HL^- \rightleftarrows FeL^+ + H^+$ have been obtained from spectrophotometric measurements. The rates of reaction are strongly affected by acidity, and the mechanism involves Fe^{3+} and $FeOH^{2+}$ metal species as well as H_2L and HL^- ligand species. The ligand acidity affects the relative importance of each path, and the results are discussed with reference to the associative/dissociative character of the reaction in relation to the metal species.

Introduction

The mechanism for the formation of labile metal complexes is generally well established in the case of divalent cations,[1] and, according to the Eigen-Tamm mechanism,[2] the rate is determined by the rate of water exchange at the inner coordination sphere of the metal.

However, no clear assessment has been achieved in the case of trivalent metal ions.[3] Moreover in this case higher positive charges and low ionic radii give increased metal-coordinated water interactions with easier proton releases and strong tendencies to hydrolysis. Therefore, the number of active species, e.g., Me^{3+} and $MeOH^{2+}$, increase and make the mechanistic interpretation more complex.

In fact, if the ligand species participates in acid-base equilibria, different reaction paths with the same dependence on acidity give rise to "proton ambiguities".[4] In addition the presence of the OH^- ligand in several cases, even if not in general, causes increased labilities and therefore increased rates are found as in the case, for example, of Al^{3+},[5] Ga^{3+},[6] Mn^{3+},[7] or Cr^{3+}.[8] In the case of Fe(III), the OH^- ligand increases by about 3 orders of magnitude the rate of water exchange of the unhydrolyzed metal and gives a dissociative character to the metal center.[9] The rate enhancement in the hydrolyzed species depresses the relative importance of the Fe^{3+} contribution in reactions with several ligands of different structure and basicity; for several ligands such as, for example, α-hydroxycarboxylic acids[9,10] or phenolic and diphenolic compounds,[11,12] the $FeOH^{2+}$ species is almost entirely the only active metal species.

For this reason few kinetic data on the unhydrolyzed species Fe^{3+} are available, and its behavior is still an object of discussion. Therefore we have undertaken a mechanistic study on the reactions of Fe(III) with a series of substituted salicylic acids, namely, 5-chloro- (Cl(SAL)), 5-nitro- (N(SAL)), 6-hydroxy- (OH(SAL)), and 3,5-dinitrosalicylic acid (DN(SAL)).

The results give information on the effect of ligand basicity on the reaction rates of the active species. In fact the sub-

* To whom correspondence should be addressed at the University of Turin.

(1) Wilkins, R. G. "The Study of Kinetics and Mechanism of Transition Metal Ion Complexes"; Allyn and Bacon: Boston, 1974.
(2) See, for example, ref 1 or: Eigen, M. "Advances in the Chemistry of the Coordination Compounds"; Kirschner, S., Ed.; Macmillan: New York, 1961; p 371.
(3) Perlmutter-Hayman, B.; Tapuhi, E. *J. Coord. Chem.* **1976**, *6*, 31.
(4) Gouger, S.; Stuehr, J. *Inorg. Chem.* **1974**, *13*, 379.
(5) Secco, F.; Venturini, M. *Inorg. Chem.* **1975**, *14*, 1978.
(6) Perlmutter-Hayman, B.; Secco, F.; Tapuhi, E.; Venturini, M. *J. Chem. Soc., Dalton Trans.* **1980**, 1124.
(7) Pelizzetti, E.; Mentasti, E.; Giraudi, G. *Inorg. Chim. Acta* **1975**, *15*, L1.
(8) Krishnamoorthy, C. R.; Harris, G. M. *J. Coord. Chem.* **1980**, *10*, 55.
(9) Mentasti, E. *Inorg. Chem.* **1979**, *18*, 1512.
(10) Mentasti, E.; Baiocchi, C. *J. Coord. Chem.* **1980**, *10*, 229.
(11) Cavasino, F. P.; Di Dio E. *J. Chem. Soc. A* **1970**, 1151.
(12) Mentasti, E.; Pelizzetti, E. *J. Chem. Soc., Dalton Trans.* **1973**, 2605.

0020-1669/82/1321-0602$01.25/0